International Journal of Pharmaceutics, 86 (1989) 211–219

IJP 02904

Solid-state properties of drugs. II. Peak shape analysis and deconvolution of overlapping endotherms in differential scanning calorimetry of chiral mixtures

M. Elsabee [b] and R.J. Prankerd [a]

[a] *Department of Pharmaceutics, College of Pharmacy, University of Florida, J. Hillis Miller Health Center, Gainesville, FL 32610 (USA) and* [b] *Department of Chemistry, University of Cairo, Cairo (Egypt)*

(Received 10 December 1991)
(Modified version received 11 May 1992)
(Accepted 12 May 1992)

Key words: DSC; Gaussian distribution; Exponentially modified Gaussian distribution; Enthalpy of fusion; Deconvolution; Solid-liquid phase diagram; Chiral drug; Minor component detection

Summary

A method for peak shape analysis and deconvolution of overlapping endotherms in differential scanning calorimetry (DSC) data is presented. The method employed a commercial computer program (PeakFit®), which fits the experimental data to two (or more) overlapping distribution functions in which heat flux is the dependent variable and temperature is the independent variable. The endotherms were found to have either Gaussian or exponentially modified Gaussian distributions. In the examples given here, a very pure reference material, benzoic acid, and a slightly impure (99.9%) sample of (±)-ephedrine hydrochloride gave single Gaussian peak shapes, whereas a slightly impure (99.9%) sample of (1*R*,2*S*)-(−)-ephedrine hydrochloride displayed a single exponentially modified Gaussian peak. Binary mixtures of (1*S*,2*R*)-(+)- and (1*R*,2*S*)-(−)-ephedrine hydrochloride gave two overlapping peaks, both of which had exponentially modified Gaussian distributions. Deconvolution of these overlapping peaks allowed construction of a solid-liquid phase diagram based on their enthalpies of fusion. This phase diagram consisted of linear plots which are easily interpolated or extrapolated. Detection of one isomer in the presence of a large excess of the other by DSC was possible for compositions containing 1.5 mol% of the minor component.

Introduction

The use of solid-liquid phase diagrams for examining binary drug-drug and drug-excipient complexation or interaction in the solid state is well established (Sekiguchi et al., 1963; Guillory et al., 1969) although it has received less attention recently (Prankerd and Ahmed, 1992). Such diagrams are usually constructed from plots of freezing temperature ('liquidus temperature') and fusion temperature ('solidus temperature') as a function of the mole fraction composition of the binary mixture. It has been demonstrated that a phase diagram constructed from the enthalpy change for fusion (ΔH_f^m) of the eutectic endotherms from a series of differential scanning calorimetry (DSC) experiments is a simple linear

Correspondence to: R.J. Prankerd, Department of Pharmacy, University of Queensland, St. Lucia, Brisbane, QLD 4072, Australia.

function of composition (Prankerd and Ahmed, 1992). Such diagrams are easier to interpret, as diagrams constructed from liquidus temperatures are very often non-linear (Patel and Hurwitz, 1972). This is also the case in systems involving interaction between the components of a mixture to form a stoichiometric complex (Guillory et al., 1969). However, estimation of the ΔH_f^m value requires that the peak of interest (i.e., the endotherm corresponding to fusion of the eutectic or the complex) be separate from any other peaks in the scan. Often, this is not the case (Botha and Lötter, 1989). Although estimation of the total ΔH_f^m for the overlapping peaks is readily performed, it is not easy to estimate the value for each individual peak. Endotherm overlapping is also commonly seen in systems of biophysical interest, such as membrane lipids (Silvius et al., 1985; Ishinaga et al., 1987). This paper presents an approach to overlapping endotherm deconvolution in pharmaceutically relevant applications.

This study used a microcomputer curve-fitting program which fitted the experimental x, y data (i.e., temperature-heat flux data) to a curve which is the sum of two or more curves of defined peak shape. The shape does not need to be the same for each peak. For physicochemical transitions such as fusion, the theoretical peak shape is a symmetrical Gaussian distribution (Eqn 1):

$$y = a_0 \exp\left[-z^2/2\right] \tag{1}$$

where y is the measured heat flux for each temperature point on the DSC scan, a_0 denotes the peak amplitude and z is a scaled representation of the x value as defined in Eqn 2:

$$z = \frac{x - a_1}{a_2} \tag{2}$$

where x represents the temperature for each heat flux measurement, a_1 is the x value corresponding to the peak center and a_2 provides a measure of peak width, the standard deviation (Jansson, 1984). This function is commonly used in deconvolution of overlapping peaks in molecular spectroscopy and in scanning microcalorimetry of protein solutions. However, most DSC scans of solids which give single peaks have an asymmetrical shape, due to premelting from impurities. This could be modelled with an exponentially modified Gaussian distribution (Eqn. 3):

$$y = f(x) = a_0 \exp\left[\frac{a_2^2}{2a_3^2} + \frac{a_1 - x}{a_3}\right] \times \left[\mathrm{erf}\left\{\frac{x - a_1}{\sqrt{2}\,a_2} - \frac{a_2}{\sqrt{2}\,a_3}\right\} + 1\right] \tag{3}$$

where the peak area $= 2a_0a_3$, a_3 is an asymmetry factor and erf{} denotes an error function. This type of distribution has been used in chromatographic applications (Yau, 1977; Foley and Dorsey, 1983; Jonsson, 1987). The approach presented here has been used in deconvolution of overlapping peaks in HPLC, but does not appear to have been applied to DSC of solids. To establish the utility of the approach, well-characterized substances (benzoic acid and ephedrine hydrochloride) have been investigated initially.

Materials and Methods

Benzoic acid (high purity thermochemical standard referenced to NBS standards, Fisher, ORM-E NA 9094, lot 855958A, ≮99.99%), (±)-, (1*S*,2*R*)-(+)- and (1*R*,2*S*)-(−)-ephedrine hydrochloride (99%, Aldrich) were used as received. Physical mixtures of finely powdered (1*S*,2*R*)-(+)- and (1*R*,2*S*)-(−)-ephedrine hydrochloride were prepared by very thorough grinding of accurately weighed (Cahn Model 2000 electromicrobalance) quantities of each isomer with an agate mortar and pestle.

DSC was performed in aluminum volatile sample pans with a Perkin-Elmer DSC-7 scanning calorimeter, a Perkin-Elmer TAC-7 controller and an IBM PS/2 Model 50 Z microcomputer (equipped with an Intel 80287 floating point coprocessor). The DSC software were P-E DSC-7 PC Series Standard Software Kit, Version 2.00, Revision 0 and P-E PC Series DSC-7 Purity Program 1, Version 2.0, Revision A. The instrument was periodically recalibrated for accuracy of on-

set temperature (T_{onset}) with indium and zinc standards and for enthalpy change (area under the fusion curve, ΔH_f^m) with indium. Scans were usually obtained for each compound at a heating rate of 2.0 K/min. Sample weights were 1.5–3 mg of the finely powdered compound and the sample holders were purged by a stream of dry nitrogen (30 cm^3/min). Before each scan, a baseline was recorded at the same heating rate and then subtracted from the experimental scan. ΔH_f^m values were obtained for the total area under each scan.

For each scan, the DSC-7 software generated a text file beginning with a data header including the starting (T_{init}) and ending (T_{final}) temperatures for the scan, and the total number of data points (N). Following the header were the data points themselves, consisting of a single column of heat flux values in mW (i.e., the y-axis). This data format was altered to be read by the curve-fitting program, which is most conveniently used with data in the form of an x, y table. The DSC-7 datafiles were read into a spreadsheet program. The values for T_{init}, T_{final} and N were used to generate a column of x-axis values ($T_n = T_{init} + n[T_{final} - T_{init}]/N$, where T_n is the n-th temperature). The y-axis values were then copied into the next column. The two columns were then copied to a new datafile (one for each DSC data set), which began with a header consisting of three rows (title of dataset, title of x-axis and title of y-axis).

The datafiles generated with the spreadsheet were then read by the curve-fitting program, PeakFit® (Version 2.0, Jandel Scientific, Corte Madera, CA). This is a simultaneous multiple non-linear curve-fitting program which uses the Marquardt-Levenberg algorithm to minimize the sum of squares of the deviations between a calculated summation curve and the observed data points (Marquardt, 1963). A total of 44 parameters could be fitted simultaneously. Up to five parameters are allowed for each of eight non-linear equations (i.e., up to eight overlapping peaks), as well as a linear or polynomial background. The power of the program is in its sophisticated graphic interface. This allows the user to quickly decide how many individual peaks are needed, and to estimate the best initial values for their parameters while directly observing the effects of any changes on the individual curves and the overall summation curve. The user is thus able to visually estimate a close approximation to the correct parameters and reduce the possibility of locating an unwanted local minimum. During fitting, the experimental data points are displayed with the individual curves and the summation curve for each iteration. Also displayed are running values for the coefficient of determination (R^2), the sum of squares and the overall F value.

In the present study, DSC scans displayed one or two endotherms. These were fitted to either Gaussian or exponentially modified Gaussian (EMG) peak distributions. Other available symmetrical peak shapes (i.e., Lorentzian, Voigt or Pearson VII distributions) gave poorer fits to the data. The asymmetry factor and error function described in Eqn 3 only accommodate asymmetric data which are skewed to the right, whereas

TABLE 1

PeakFit parameters for benzoic acid using Gaussian and EMG models

Parameter	Value	S.E.	t value	Upper 95% c.i.	Lower 95% c.i.
Gaussian model (F = 133218)					
a_0	8075.16134	13.024	620.003	8049.53	8100.79
a_1	123.2689	0.00118	1.0437e + 6	123.271	123.267
a_2	0.6341	0.001181	536.943	0.6318	0.6365
EMG model (F = 94887)					
a_0	33576.99	2670.0710	12.575	28322.26	38831.71
a_1	123.452	0.01357	9095.947	123.479	123.425
a_2	0.60858	0.00400	152.063	0.60071	0.61646
a_3	0.19067	0.01522	12.525	0.16071	0.22063

asymmetric DSC scans in their normal representation are skewed to the left. It was therefore necessary to multiply all x values by -1 to obtain x, y data with the correct direction of skew. All fitted parameters in which the factor of -1 appeared were corrected after fitting to give the proper DSC representation. The best fit was decided by the highest t values and overall F value for the regression and the narrowest 95% confidence intervals (95% c.i.) for the individual parameters. The coefficient of determination (R^2) is not an acceptable criterion for goodness of fit, unless the number of degrees of freedom remains constant for all comparisons. This is not usually the case.

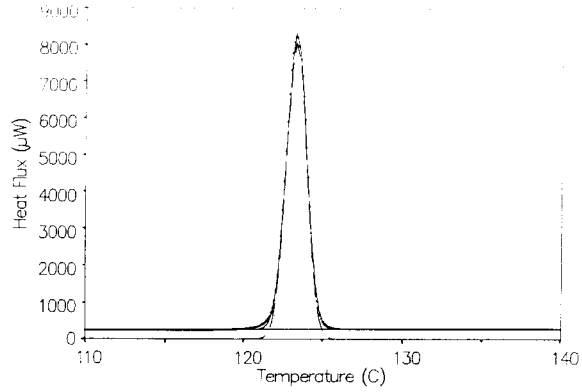

Fig. 1. PeakFit plot of DSC data for high purity benzoic acid: (·····) experimental points; (— — —) Gaussian curve; (———) summation curve (Gaussian plus linear background).

Results and Discussion

Peak shapes for DSC scans of single substances

A highly pure sample of benzoic acid gave a single DSC peak which was better described by a Gaussian distribution (Table 1 and Fig. 1). These data demonstrate that the Gaussian distribution fitted the experimental data better than the EMG distribution, although the EMG distribution gave a satisfactory fit. The overall F ratio is higher for the Gaussian fit and the 95% c.i. for the parameters are very narrow. For the EMG fit, the standard errors for a_0 and a_3 are large, their t values are small, and these parameters have wide 95% confidence intervals. Fig. 1 shows that the only discrepancy between the observed data points and the theoretical line is a statistically insignificant asymmetry on the leading edge of the endotherm.

A DSC scan of (±)-ephedrine hydrochloride gave a single endotherm which was better described by a Gaussian distribution (Table 2 and Fig. 2), although the EMG distribution also fitted the endotherm. These data indicate that both distributions fit the data well, although the Gaussian fit is better, as the F ratio and t values are larger, and the 95% c.i. are small. (1*R*,2*S*)-(−)-Ephedrine hydrochloride gave an endotherm which was better described by an EMG distribution (Table 3 and Fig. 3).

The data in Table 3 demonstrate that the EMG distribution fitted the experimental data far better than the Gaussian distribution. The overall F ratio is much higher for the EMG fit

TABLE 2

PeakFit parameters for (±)-ephedrine hydrochloride using Gaussian and EMG models

Parameter	Value	S.E.	t value	Upper 95% c.i.	Lower 95% c.i.
Gaussian model (F = 8116)					
a_0	482.585	3.1885	151.353	476.291	488.880
a_1	188.212	0.003876	4.8557*e* + 5	188.204	188.220
a_2	0.5081	0.003876	131.075	0.5004	0.5157
EMG model (F = 6642)					
a_0	1523.13	232.868	6.5408	1063.39	1982.87
a_1	188.401	0.02605	7.2336*e* + 3	188.35	188.45
a_2	0.4748	0.01005	47.240	0.4549	0.4946
a_3	0.2026	0.03128	6.4765	0.1409	0.2644

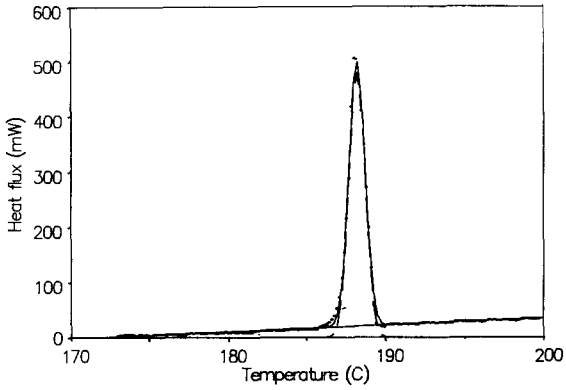

Fig. 2. PeakFit plot of DSC data for (±)-ephedrine hydrochloride: (· · · · · ·) experimental points; (— — —) Gaussian curve: (———) summation curve (Gaussian plus linear background).

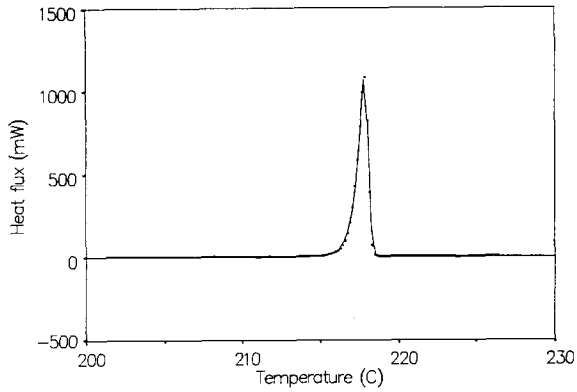

Fig. 3. PeakFit plot of DSC data for (1*R*,2*S*)-(−)-ephedrine hydrochloride: (· · · · · ·) experimental points; (———) EMG curve.

and the 95% c.i. for the parameters are very narrow. The mole percent purities for both (±)- and (1*R*,2*S*)-(−)-ephedrine hydrochloride estimated by the DSC-7 software were greater than 99.9% (Wendlandt, 1986). There is no inconsistency in that (±)-ephedrine hydrochloride was better fitted by a Gaussian curve while (1*R*,2*S*)-(−)-ephedrine hydrochloride was better fitted by an EMG curve. This merely suggests that the level of impurity was slightly greater for the sample of the (1*R*,2*S*)-(−)- diastereomer.

Deconvolution of overlapping endotherms in DSC scans of binary mixtures

DSC scans of physical mixtures of (1*S*,2*R*)-(+)- and (1*R*,2*S*)-(−)-ephedrine hydrochloride displayed two endotherms which overlapped when the mole percent of one optical isomer was from 5 to 95%. From 35 to 65%, the two peaks were superimposed, appearing as a single peak with a very broad base (Fig. 4). The above approach was used to deconvolute the two peaks. Both endotherms of each scan were fitted better by the EMG distribution. The ratio of each peak area to

TABLE 3

PeakFit parameters for (1R,2S)-(−)-ephedrine hydrochloride using Gaussian and EMG models

Parameter	Value	S.E.	*t* value	Upper 95% c.i.	Lower 95% c.i.
Gaussian model (F = 2084)					
a_0	1024.82	18.824	54.443	987.64	1062.00
a_1	217.709	0.007347	2.9634e + 4	217.694	217.724
a_2	0.3464	0.007347	47.150	0.3319	0.3609
EMG model (F = 61445)					
a_0	1018.91	6.6997	152.08	1005.68	1032.15
a_1	218.0189	0.00145	1.5014e + 5	218.016	218.021
a_2	0.18392	0.00156	117.829	0.1808	0.1870
a_3	0.47407	0.00368	128.871	0.4668	0.4813

the total area was used to apportion the total enthalpy of fusion, previously calculated by the DSC-7 software.

All F ratios reported in Table 4 represent highly significant fits to the experimental data ($p < 0.001$ in the worst case) (Rohlf and Sokal, 1969). The peak center (a_1) values in Table 4 are virtually constant for the lower melting of the two endotherms (peak 1). This corresponds to melting of the racemic mixture. For the two physical compositions nearest to the racemic mixture (49.60 and 54.99% (1*R*,2*S*)-(−)-ephedrine hydrochloride), the program could only distinguish a single endotherm with an EMG distribution. Where present, the higher melting endotherm (peak 2) corresponds to the isomer in excess, for which the peak amplitude (a_0) and peak center (a_1) are maximal when no racemic mixture is present, i.e., there is only a single isomer present. The relative area for peak 1 increases as the composition of the physical mixture approaches the racemic mixture. These relative areas were used to calculate the changes in enthalpy of fusion (ΔH_f^m) for the two peaks that are reported in Table 5 and plotted as a function of mol% composition in Fig. 5. Table 5 and Fig. 5 also report the temperature for which melting is completed (liquidus temperature) for each composition.

The data in Table 5 show that addition of one isomer to the other results in DSC endotherms corresponding to the isomer in excess and the racemic mixture. For low mol% compositions of one isomer in the other, the appearance of the

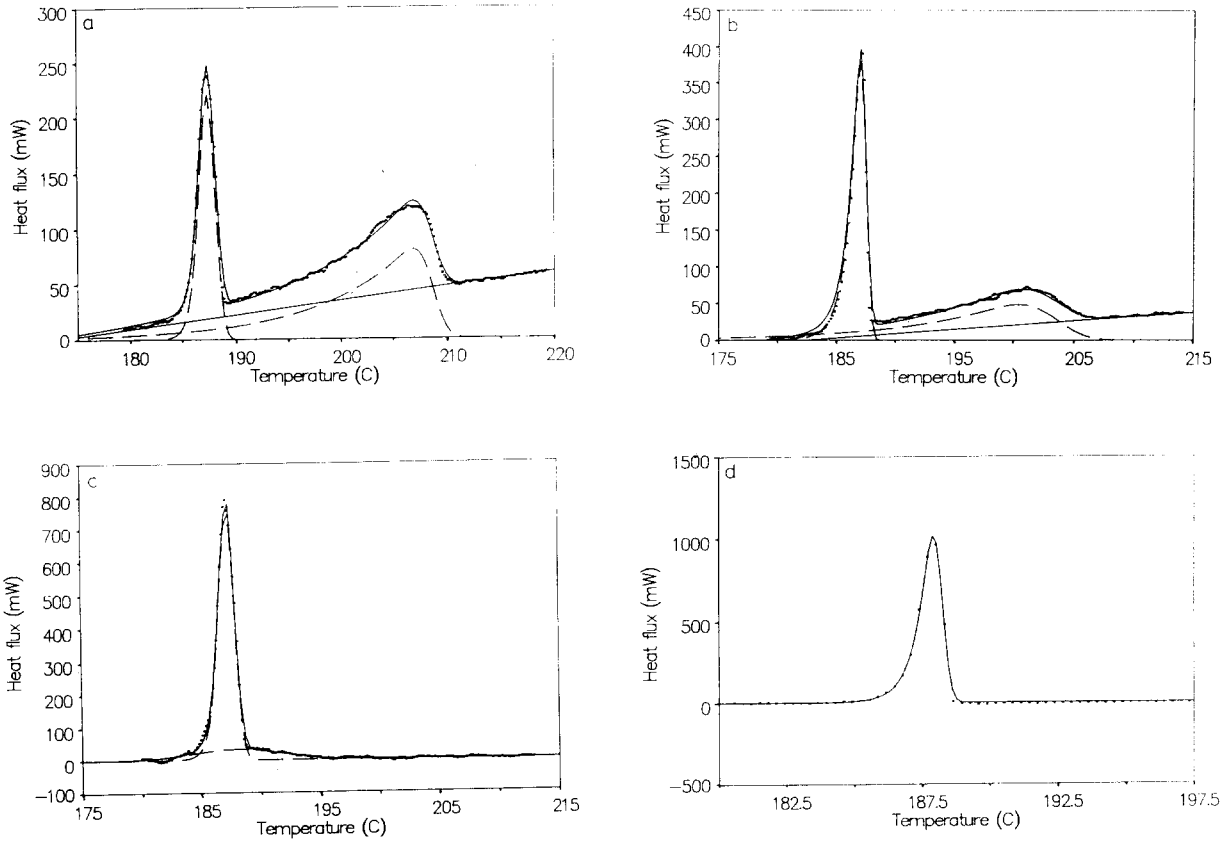

Fig. 4. PeakFit plots of DSC data for physical mixtures of (1*R*,2*S*)-(−)- and (1*S*,2*R*)-(+)-ephedrine hydrochloride: (a) 13.99 mol% (1*R*,2*S*)-(−)-; (b) 20.00 mol% (1*R*,2*S*)-(−)-; (c) 36.10 mol% (1*R*,2*S*)-(−)-; (d) 49.60 mol% (1*R*,2*S*)-(−)-. (· · · · · ·) Experimental points; (— — —) EMG curves; (———) summation curve (EMG curves plus linear background).

racemic mixture endotherm indicates that detection of small quantities of the minor component (1.5 mol% or even less) is not difficult. Similar examples have been reported very recently (Bettinetti et al., 1990; Pitrè et al., 1991). Detection of low levels of enantiomeric impurities from the DSC scan is rapid (20–30 min). Further evaluation of the use of DSC in estimation of enantiomeric purity will be the subject of a later article in this series. The phenomenon of eutectic melting should be of general applicability to enantiomeric mixtures, and should have applications in the quality control of raw materials in the pharmaceutical industry. An additional factor is that the development of stereospecific HPLC separations of enantiomers is often time-consuming (Karnik et al., 1991), and may even require chiral derivatization to form diastereomers. It is expected that these two approaches to chiral impurity detection should complement each other, and may be especially important where the enantiomers have different or opposing pharmacological activities (Pitrè et al., 1991). Detection and quantification of small amounts of one enantiomer in another by the DSC method would be expected to fail only in the unusual case of the formation of a racemic solid solution, or where decomposition of the melt was rapid.

The symmetrical phase diagram illustrated in Fig. 5 is consistent with the formation of a simple eutectic when (1*S*,2*R*)-(+)- and (1*R*,2*S*)-(−)-ephedrine hydrochloride are physically mixed, i.e., a true racemic mixture consisting of minute crystals of each pure diastereomer is present (conglomerate). Formation of a racemic compound (intermolecular complex) would result in a more complex phase diagram containing two eutectic points. Systems giving this behavior will be the subject of a later paper in this series. Plotting of ΔH_f^m values as a function of mol% composition results in linear plots which are easier to interpolate and extrapolate than the traditional plots of liquidus and solidus temperatures, which are often curved (Patel and Hurwitz, 1972; Prankerd and Ahmed, 1992).

TABLE 4

Peak centers (a_1) and relative endotherm areas for DSC scans of physical mixtures of (1S,2R)-(+)- and (1R,2S)-(−)-ephedrine hydrochloride using the EMG model

% (1*R*,2*S*)-(−)-	*F* ratio	a_1 (peak 1) (°C)	Relative area (peak 1)	a_1 (peak 2) (°C)	Relative area (peak 2)
0.00		–	–	214.0	1.000
5.09	3268	187.2	0.1264	214.0	0.8736
13.99	4707	187.7	0.3356	208.6	0.6644
20.00	825	187.4	0.5203	203.3	0.4797
36.10	11562	187.2	0.8140	188.2	0.1860
39.70	1359	187.6	0.9887	188.9	0.0113
49.60	5868	187.9	1.000	–	–
50.00 [a]	6643	188.2	1.000	–	–
54.99	4170	187.7	1.000	–	–
61.54	9888	187.2	0.9646	189.0	0.0354
74.93	11180	187.6	0.5506	200.8	0.4494
84.26	5975	187.5	0.3541	207.3	0.6459
89.53	2390	187.1	0.1959	211.8	0.8041
92.57	6906	187.2	0.1820	212.5	0.8180
94.90	11992	187.1	0.1322	213.6	0.6878
100.0	61445	–	–	218.0	1.000

[a] Pure racemic (±)-ephedrine hydrochloride.

TABLE 5

Changes in enthalpies for fusion (ΔH_f^m, J g^{-1}) based on the relative areas in Table 4 and liquidus temperatures from DSC scans of physical mixtures of (1S,2R)-(+)- and (1R,2S)-(−)-ephedrine hydrochloride

% (1R,2S)-(−)-	ΔH_f^m (peak 1)	ΔH_f^m (peak 2)	Liquidus temperature
0.00	–	166.34	216.5
2.60 [b]	5.90	145.13	216.2
5.09	20.59	142.27	214.6
13.99	55.68	110.24	210.0
20.00	75.66	82.08	206.0
36.10	137.18	31.35	200.0
39.70	157.63	1.79	191.7
49.60	166.97	–	188.8
50.00 [a]	178.93	–	188.5
54.99	168.00	–	189.0
61.54	156.58	5.74	192.0
74.93	91.46	74.66	203.8
84.26	59.72	108.92	209.1
89.53	33.20	136.53	212.6
92.57	28.42	127.75	212.9
94.90	21.07	138.31	214.3
96.34 [b]	12.38	151.56	215.3
98.51 [b]	5.21	153.77	217.2
100.0	–	171.01	218.4

[a] Pure racemic (±)-ephedrine hydrochloride.

[b] Endotherms had baseline separation and did not require deconvolution.

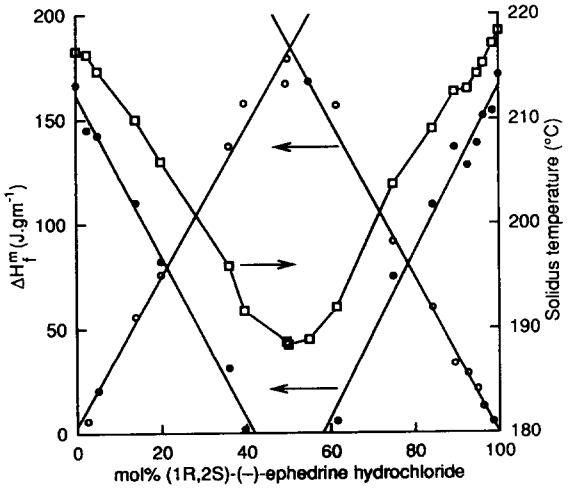

Fig. 5. ΔH_f^m values for the racemic mixture (○) and diastereomers (●) and the corresponding liquidus temperatures (□) as a function of mol% (1R,2S)-(−)-ephedrine hydrochloride in physical mixtures of the two diastereomers.

Acknowledgements

This study was funded by a University of Florida DSR Research Development Award. Additional financial support was given by Smith-Kline Beecham.

References

Bettinetti, G., Giordano, F., Fronza, G., Italia, A., Pellegata, R., Villa, M. and Ventura, P., Sobrerol enantiomers and racemates: Solid state spectroscopy, thermal behavior and phase diagrams. *J. Pharm. Sci.*, 79 (1990) 470–475.

Botha, S.A. and Lötter, A.P., Compatibility study between exprenolol hydrochloride and tablet excipients using differential scanning calorimetry. *Drug Dev. Ind. Pharm.*, 15 (1989) 1843–1853.

Foley, J.P. and Dorsey, J.G., Equations for calculation of chromatographic figures of merit for ideal and skewed peaks. *Anal. Chem.*, 55 (1983) 730–737.

Guillory, J.K., Hwang, S.C. and Lach, J.L., Interactions between pharmaceutical compounds by thermal methods. *J. Pharm. Sci.*, 58 (1969) 301–308.

Ishinaga, M., Mukai, K., Suemune, N. and Asai, M., Effects of propyl gallate on the phospholipid composition of *Escherichia coli* and the thermotropic behavior of lipids. *Agric. Biol. Chem.*, 51 (1987) 483–487.

Jansson, P.A., *Deconvolution with Applications in Spectroscopy*, Academic Press, New York, 1984.

Jonsson, J.A., *Chromatographic Theory and Basic Principles*, Dekker, New York, 1987.

Karnik, N.A., Prankerd, R.J. and Perrin, J.H., Fluorometric and liquid chromatographic study of the binding of two coumarins to β-cyclodextrin. *Chirality*, 3 (1991) 124–128.

Marquardt, D.W., An algorithm for least squares estimation of non-linear parameters. *J. Soc. Indust. Appl. Math.*, 11 (1963) 431–441.

Patel, R.M. and Hurwitz, A., Eutectic temperature determination of preformulation systems and evaluation by controlled freeze drying. *J. Pharm. Sci.*, 61 (1972) 1806–1810.

Pitrè, D., Nebuloni, M. and Ferri, V., Calorimetric determination of the enantiomeric purity of (1*R*, 2*R*)-2-amino-1-(4-nitrophenyl)-1,3-propanediol. *Arch. Pharm. (Weinheim)*, 324 (1991) 325–328.

Prankerd, R.J. and Ahmed, S.M., Physicochemical interactions involving praziquantel, oxamniquine and tablet excipients. *J. Pharm. Pharmacol.*, 44 (1992) 259–261.

Rohlf, F.J. and Sokal, R.R., *Statistical Tables*, Freeman, San Francisco, 1969, pp. 168–197.

Sekiguchi, K., Ueda, Y. and Nakamori, Y., Studies on the method of thermal analysis of organic medicinals. *Chem. Pharm. Bull.*, 11 (1963) 1108–1112.

Silvius, J.R., Lyons, M., Yeagle, P.L. and O'Leary, T.J., Thermotropic properties of bilayers containing branched-chain phospholipids. *Biochemistry*, 24 (1985) 5388–5395.

Wendlandt, W.W., *Thermal Analysis*, Wiley, New York, 1986, Ch. 10.

Yau, W.W., Characterizing skewed chromatographic band broadening. *Anal. Chem.*, 49 (1977) 395–398.